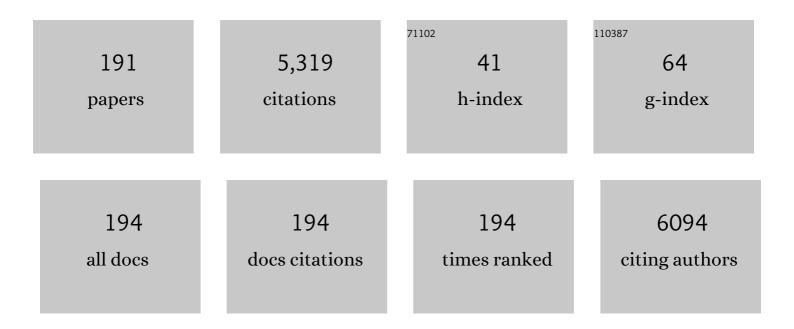
List of Publications by Year in descending order

Source: https://exaly.com/author-pdf/873302/publications.pdf Version: 2024-02-01



FIDED DE LA ROSA

#	Article	IF	CITATIONS
1	Towards translation of surface-enhanced Raman spectroscopy (SERS) to clinical practice: Progress and trends. TrAC - Trends in Analytical Chemistry, 2021, 134, 116122.	11.4	62
2	Imaging and SERS Study of the Au Nanoparticles Interaction with HPV and Carcinogenic Cervical Tissues. Molecules, 2021, 26, 3758.	3.8	5
3	Ligand-targeted Theranostic Liposomes combining methylene blue attached upconversion nanoparticles for NIR activated bioimaging and photodynamic therapy against HER-2 positive breast cancer. Journal of Luminescence, 2021, 237, 118143.	3.1	17
4	Anti-fouling SERS-based immunosensor for point-of-care detection of the B7–H6 tumor biomarker in cervical cancer patient serum. Analytica Chimica Acta, 2020, 1138, 110-122.	5.4	38
5	Stealth modified bottom up SERS substrates for label-free therapeutic drug monitoring of doxorubicin in blood serum. Talanta, 2020, 218, 121138.	5.5	24
6	Improving the stability of perovskite solar cells under harsh environmental conditions. Solar Energy, 2020, 202, 438-445.	6.1	12
7	Enhanced Raman Effect of Solvothermal Synthesized Reduced Graphene Oxide/Titanium Dioxide Nanocomposites. ChemistrySelect, 2020, 5, 3789-3797.	1.5	4
8	A Turn-On Luminescence Method for Phosphate Determination Based on Fast Green-Functionalized ZrO ₂ :Yb,Er@ZrO ₂ Core@Shell Upconversion Nanoparticles. Analytical Chemistry, 2019, 91, 14657-14665.	6.5	18
9	Theranostic nanocomplex of gold-decorated upconversion nanoparticles for optical imaging and temperature-controlled photothermal therapy. Journal of Photochemistry and Photobiology A: Chemistry, 2019, 384, 112053.	3.9	17
10	Study of inverted planar CH3NH3PbI3 perovskite solar cells fabricated under environmental conditions. Solar Energy, 2019, 180, 594-600.	6.1	11
11	Role of carbon nanodots in defect passivation and photo-sensitization of mesoscopic-TiO2 for perovskite solar cells. Carbon, 2019, 146, 388-398.	10.3	33
12	Controlling trapping states on selective theranostic core@shell (NaYF ₄ :Yb,Tm@TiO ₂ -ZrO ₂) nanocomplexes for enhanced NIR-activated photodynamic therapy against breast cancer cells. Dalton Transactions, 2019, 48, 9962-9973.	3.3	23
13	Co-sensitized TiO2 electrodes with different quantum dots for enhanced hydrogen evolution in photoelectrochemical cells. Journal of Applied Electrochemistry, 2019, 49, 475-484.	2.9	4
14	Novel anti-HER2 peptide-conjugated theranostic nanoliposomes combining NaYF ₄ :Yb,Er nanoparticles for NIR-activated bioimaging and chemo-photodynamic therapy against breast cancer. Nanoscale, 2019, 11, 20598-20613.	5.6	37
15	Ultrasensitive SERS Substrate for Label-Free Therapeutic-Drug Monitoring of Paclitaxel and Cyclophosphamide in Blood Serum. Analytical Chemistry, 2019, 91, 2100-2111.	6.5	67
16	Light-induced effects on crystal size and photo-stability of colloidal CsPbBr ₃ perovskite nanocrystals. Materials Research Express, 2019, 6, 045041.	1.6	19
17	Improved performance of inverted planar MAPbI3 based perovskite solar cells using bromide post-synthesis treatment. Solar Energy, 2019, 177, 538-544.	6.1	10
18	Eu ³⁺ â€doped glass as a color rendering index enhancer in phosphorâ€inâ€glass. Journal of the American Ceramic Society, 2018, 101, 2914-2920.	3.8	11

#	Article	lF	CITATIONS
19	Improving the Optoelectronic Properties of Mesoporous TiO ₂ by Cobalt Doping for High-Performance Hysteresis-free Perovskite Solar Cells. ACS Applied Materials & Interfaces, 2018, 10, 3571-3580.	8.0	78
20	An immunoconjugated up-conversion nanocomplex for selective imaging and photodynamic therapy against HER2-positive breast cancer. Nanoscale, 2018, 10, 10154-10165.	5.6	35
21	Effect of BaF 2 addition on luminescence properties of Er 3+ /Yb 3+ co-doped phosphate glasses. Journal of Rare Earths, 2018, 36, 58-63.	4.8	21
22	Interfacial Engineering of TiO ₂ by Graphene Nanoplatelets for High-Efficiency Hysteresis-free Perovskite Solar Cells. ACS Sustainable Chemistry and Engineering, 2018, 6, 15391-15401.	6.7	18
23	Hydrothermal synthesis of graphene oxide/multiform hydroxyapatite nanocomposite: its influence on cell cytotoxicity. Materials Research Express, 2018, 5, 125023.	1.6	7
24	Improved performance of CdS quantum dot sensitized solar cell by solvent modified SILAR approach. Solar Energy, 2018, 174, 240-247.	6.1	28
25	Synthesis and characterization of Fe3O4:Yb3+:Er3+ nanoparticles with magnetic and optical properties for hyperthermia applications. Journal of Magnetism and Magnetic Materials, 2018, 465, 406-411.	2.3	11
26	Modulating the grain size, phase and optoelectronic quality of perovskite films with cesium iodide for high-performance solar cells. Journal of Materials Chemistry C, 2018, 6, 7880-7889.	5.5	21
27	The synthesis of transparent TiO2 photoelectrodes assisted by rheological agent (triton x-100, PVP) Tj ETQq1 1	0.784314 0.8	rgॺॖॖॖT /Overloc
28	Study of ethoxyethane deposition time and Co (III) complex doping on the performance of mesoscopic perovskite based solar cells. Solar Energy Materials and Solar Cells, 2017, 163, 224-230.	6.2	14
29	Enhanced Photovoltaic Performance of Mesoscopic Perovskite Solar Cells by Controlling the Interaction between CH ₃ NH ₃ Pbl ₃ Films and CsPbX ₃ Perovskite Nanoparticles. Journal of Physical Chemistry C, 2017, 121, 4239-4245.	3.1	42
30	Luminance enhancement in quantum dot light-emitting diodes fabricated with Field's metal as the cathode. Journal Physics D: Applied Physics, 2017, 50, 095106.	2.8	1
31	Synthesis of co-doped Yb 3+ -Er 3+ :ZrO 2 upconversion nanoparticles and their applications in enhanced photovoltaic properties of quantum dot sensitized solar cells. Journal of Alloys and Compounds, 2017, 698, 433-441.	5.5	44
32	Studying the role of CdS on the TiO2 surface passivation to improve CdSeTe quantum dots sensitized solar cell. Journal of Alloys and Compounds, 2017, 728, 1058-1064.	5.5	22
33	Tuning Color Temperature of White OLEDs in Parallel Tandems. Physica Status Solidi (A) Applications and Materials Science, 2017, 214, 1700283.	1.8	6
34	Improved performance of mesoscopic perovskite solar cell using an accelerated crystalline formation method. Journal of Power Sources, 2017, 365, 169-178.	7.8	17
35	Operating Mechanisms of Mesoscopic Perovskite Solar Cells through Impedance Spectroscopy and <i>J</i> – <i>V</i> Modeling. Journal of Physical Chemistry Letters, 2017, 8, 6073-6079.	4.6	69
36	Enhancement of Efficiency in Quantum Dot Sensitized Solar Cells Based on CdS/CdSe/CdSeTe Heterostructure by Improving the Light Absorption in the VIS-NIR Region. Electrochimica Acta, 2017, 247, 899-909.	5.2	37

#	Article	IF	CITATIONS
37	SERS and integrative imaging upon internalization of quantum dots into human oral epithelial cells. Journal of Biophotonics, 2016, 9, 683-693.	2.3	12
38	Interaction of TGA@CdTe Quantum Dots with an Extracellular Matrix of <i>Haematococcus pluvialis</i> Microalgae Detected Using Surface-Enhanced Raman Spectroscopy (SERS). Applied Spectroscopy, 2016, 70, 1561-1572.	2.2	6
39	Nonconventional illumination with LEDs. , 2016, , .		Ο
40	Nanomolar detection of glucose using SERS substrates fabricated with albumin coated gold nanoparticles. Nanoscale, 2016, 8, 11862-11869.	5.6	25
41	Photovoltaic study of quantum dot-sensitized TiO2/CdS/ZnS solar cell with P3HT or P3OT added. Journal of Applied Electrochemistry, 2016, 46, 975-985.	2.9	15
42	Strong enhancement of the upconversion emission in ZrO2: Yb3+, Er3+, Gd3+ nanocubes synthesized with Na2S. Journal of Luminescence, 2016, 172, 154-160.	3.1	7
43	Effect of P2O5 addition on structural and luminescence properties of Nd3+-doped tellurite glasses. Journal of Alloys and Compounds, 2016, 684, 322-327.	5.5	59
44	SERS-active Au/SiO_2 clouds in powder for rapid ex vivo breast adenocarcinoma diagnosis. Biomedical Optics Express, 2016, 7, 2407.	2.9	7
45	Effect of the electrophoretic deposition of Au NPs in the performance CdS QDs sensitized solar Cells. Electrochimica Acta, 2016, 188, 710-717.	5.2	32
46	Persistent luminescence of Eu2+ doped glass ceramic for AC LED. , 2016, , .		0
47	Efficient blue-green emission of Ce3+ doped glass ceramic. , 2016, , .		0
48	Tunable color parallel tandem organic light emitting devices with carbon nanotube and metallic sheet interlayers. Journal of Applied Physics, 2015, 118, 194502.	2.5	4
49	Influence of pH and europium concentration on the luminescent and morphological properties of Y2O3 powders. Optical Materials, 2015, 48, 97-104.	3.6	8
50	Effect of Different Sensitization Technique on the Photoconversion Efficiency of CdS Quantum Dot and CdSe Quantum Rod Sensitized TiO ₂ Solar Cells. Journal of Physical Chemistry C, 2015, 119, 13394-13403.	3.1	68
51	Spectroscopic properties of tellurite glasses co-doped with Er3+ and Yb3+. Journal of Luminescence, 2015, 162, 72-80.	3.1	42
52	Wet chemical synthesis of quantum dots for medical applications. , 2015, , .		0
53	Photovoltaic properties of multilayered quantum dot/quantum rod-sensitized TiO2 solar cells fabricated by SILAR and electrophoresis. Physical Chemistry Chemical Physics, 2015, 17, 18590-18599.	2.8	37
54	Spectroscopic properties of Eu3+/Nd3+ co-doped phosphate glasses and opaque glass–ceramics. Optical Materials, 2015, 46, 34-39.	3.6	26

#	Article	IF	CITATIONS
55	Labeling of HeLa cells using ZrO 2 : Yb 3 + - Er 3 + nanoparticles with upconversion emission. Journal of Biomedical Optics, 2015, 20, 046006.	2.6	13
56	SERS substrates fabricated with star-like gold nanoparticles for zeptomole detection of analytes. Nanoscale, 2015, 7, 10249-10258.	5.6	57
57	Current improvement in hybrid quantum dot sensitized solar cells by increased light-scattering with a polymer layer. RSC Advances, 2015, 5, 36140-36148.	3.6	18
58	Effect of TEA on the blue emission of ZnO quantum dots with high quantum yield. Optical Materials Express, 2015, 5, 1109.	3.0	24
59	Photovoltaic Properties of Bi2S3 and CdS Quantum Dot Sensitized TiO2 Solar Cells. Electrochimica Acta, 2015, 180, 486-492.	5.2	57
60	Switching green to red emission in tridoped ZrO2:Yb3+–Er3+–Bi3+ nanocrystals. Optical Materials, 2015, 48, 92-96.	3.6	10
61	Er3+ loaded barium molybdate nanoparticles: IR to visible spectral upconversion. Materials Letters, 2015, 142, 7-10.	2.6	8
62	Synthesis and optical properties of BaTiO3:Eu3+@SiO2 glass ceramic nano particles. Journal of Sol-Gel Science and Technology, 2014, 72, 435-442.	2.4	8
63	Rhodamine B Detection by SERS with Urchin-like Gold Nanostructures in Water Solution. , 2014, , .		1
64	Glucose detection using SERS with multi-branched gold nanostructures in aqueous medium. RSC Advances, 2014, 4, 59233-59241.	3.6	27
65	Characterization of a Yellow Emitting QD-LED. , 2014, , .		Ο
66	Quantum Dots Solar Cells of CdS Deposited by Chemical Bath Method. , 2014, , .		1
67	Selection criteria for SERS substrates. , 2014, , .		1
68	White light emission from a blue polymer light emitting diode combined with <scp>YAG</scp> : <scp>C</scp> e ³⁺ nanoparticles. Physica Status Solidi (A) Applications and Materials Science, 2014, 211, 651-655.	1.8	5
69	White light generation from YAG/YAM:Ce3+, Pr3+, Cr3+ nanophosphors mixed with a blue dye under 340nm excitation. Journal of Luminescence, 2014, 154, 185-192.	3.1	17
70	Understanding the infrared to visible upconversion luminescence properties of Er3+/Yb3+ co-doped BaMoO4 nanocrystals. Journal of Solid State Chemistry, 2014, 216, 36-41.	2.9	34
71	Lu2O3:Eu3+ glass ceramic films: Synthesis, structural and spectroscopic studies. Materials Research Bulletin, 2014, 51, 418-425.	5.2	12
72	Microwave hydrothermal synthesis and infrared to visible upconversion luminescence of Er3+/Yb3+ co-doped bismuth molybdate nanopowder. Journal of Luminescence, 2014, 145, 866-871.	3.1	38

#	Article	IF	CITATIONS
73	Panchromatic Solar-to-H ₂ Conversion by a Hybrid Quantum Dots–Dye Dual Absorber Tandem Device. Journal of Physical Chemistry C, 2014, 118, 891-895.	3.1	27
74	Improving pure red upconversion emission of Co-doped Y2O3:Yb3+–Er3+ nanocrystals with a combination of sodium sulfide and surfactant Pluronic-F127. Journal of Luminescence, 2014, 145, 292-298.	3.1	13
75	Photoluminescence characterization of porous YAG: Yb3+–Er3+ nanoparticles. Journal of Luminescence, 2014, 153, 21-28.	3.1	15
76	Synthesis of Lu ₂ O ₃ :Eu ³⁺ Luminescent Ceramic Powder Embedded in SiO ₂ Matrix. Materials Transactions, 2014, 55, 1867-1871.	1.2	4
77	Semi-transparent polymer light emitting diodes with multiwall carbon nanotubes as cathodes. Physica Status Solidi (A) Applications and Materials Science, 2014, 211, 2828-2832.	1.8	4
78	Upconversion emision of nanophosphors for cervical cancer detection. , 2014, , .		0
79	Yellow upconversion emission in Er/Yb codoped glass ceramic. , 2014, , .		Ο
80	Eu ³⁺ , Bi ³⁺ codoped Lu ₂ O ₃ nanopowders: Synthesis and luminescent properties. Journal of Materials Research, 2013, 28, 1365-1371.	2.6	10
81	NaOH-controlled upconversion of nanocrystalline BaZrO _{3:Er,Yb phosphor. International Journal of Nanotechnology, 2013, 10, 1055.}	0.2	2
82	Polarimetric characterization of bismuth thin films deposited by laser ablation. Applied Optics, 2012, 51, 8549.	1.8	5
83	Multicolor Upconversion Emission and Color Tunability in Tm3+/Er3+/Yb3+ Tri-Doped NaNbO3 Nanocrystals. Materials Express, 2012, 2, 294-302.	0.5	21
84	Strong blue and white photoluminescence emission of BaZrO3 undoped and lanthanide doped phosphor for light emitting diodes application. Journal of Solid State Chemistry, 2012, 196, 243-248.	2.9	29
85	Upconversion emission in a carbon-implanted Yb:YAG planar waveguide. Optics Communications, 2012, 285, 5531-5534.	2.1	7
86	Synthesis, characterization and surface enhanced Raman scattering of hollow gold–silica double shell nanostructures. Biomedical Spectroscopy and Imaging, 2012, 1, 275-291.	1.2	5
87	Comparative study of the spectroscopic properties of Yb3+/Er3+ codoped tellurite glasses modified with R2O (R=Li, Na and K). Journal of Luminescence, 2012, 132, 391-397.	3.1	26
88	Wall Rock-Like Y2O3 Nanorods by Hydrothermal Synthesis and their Luminescence Properties. Science of Advanced Materials, 2012, 4, 551-557.	0.7	8
89	A Special Issue on Optical Nanomaterials: Challenges and Opportunities. Science of Advanced Materials, 2012, 4, 549-550.	0.7	0
90	Third-order nonlinear optical response and photoluminescence characterization of tellurite glasses with different alkali metal oxides as network modifiers. Journal of Applied Physics, 2011, 110, 083110.	2.5	9

#	Article	IF	CITATIONS
91	Photovoltaic Conversion Enhancement of CdSe Quantum Dot-Sensitized TiO2 Decorated with Au Nanoparticles and P3OT. Journal of Physical Chemistry C, 2011, 115, 23209-23220.	3.1	53
92	Effect of solvent on the up- and downconversion emissions of Y_2O_3:Yb^3+â^'Er^3+ nanofibers synthesized by a hydrothermal method. Journal of the Optical Society of America B: Optical Physics, 2011, 28, 649.	2.1	7
93	Gold aggregates on silica templates and decorated silica arrays for SERS applications. European Physical Journal D, 2011, 63, 301-306.	1.3	10
94	Y2O3:Eu3+,Tb3+ thin films prepared by sol–gel method: structural and optical studies. Journal of Sol-Gel Science and Technology, 2011, 58, 366-373.	2.4	12
95	Solvent and surfactant effect on the self-assembly and luminescence properties of ZrO2:Eu3+ nanoparticles. Applied Physics B: Lasers and Optics, 2011, 102, 641-649.	2.2	17
96	Visible upconversion emission and non-radiative direct Yb3+ to Er3+ energy transfer processes in nanocrystalline ZrO2:Yb3+,Er3+. Optics and Lasers in Engineering, 2011, 49, 703-708.	3.8	20
97	Gd3+and S2+sensitizer effect on the upconversion emission of ZrO 2 :Yb3+, Er3+nanocrystals prepared by precipitation method with a hydrothermal process. , 2011, , .		1
98	Red, green, blue and white light upconversion emission in Yb3+/Tm3+/Ho3+co-doped tellurite glasses. Journal Physics D: Applied Physics, 2011, 44, 455308.	2.8	25
99	Cooperative emission in ion implanted Yb:YAG waveguides. Journal of Physics: Conference Series, 2011, 274, 012122.	0.4	1
100	Synthesis and characterization of upconversion emission on lanthanides doped ZrO 2 nanocrystals coated with SiO 2 for biological applications. Proceedings of SPIE, 2010, , .	0.8	1
101	Magnetite and magnetite/silver core/shell nanoparticles with diluted magnet-like behavior. Journal of Solid State Chemistry, 2010, 183, 99-104.	2.9	24
102	Color tunability of the upconversion emission in Er–Yb doped the wide band gap nanophosphors ZrO2 and Y2O3. Materials Science and Engineering B: Solid-State Materials for Advanced Technology, 2010, 174, 177-181.	3.5	47
103	Green and red upconverted emission of hydrothermal synthesized Y2O3: Er3+–Yb3+ nanophosphors using different solvent ratio conditions. Materials Science and Engineering B: Solid-State Materials for Advanced Technology, 2010, 174, 164-168.	3.5	29
104	Structural and luminescence characterization of silica coated Y2O3:Eu3+ nanopowders. Optical Materials, 2010, 32, 1471-1479.	3.6	21
105	High angle annular dark field-scanning transmission electron microscopy and high-resolution transmission electron microscopy studies in the Er2O3–ZrO2 system. Vacuum, 2010, 84, 1226-1231.	3.5	5
106	Room-temperature deposition of crystalline patterned ZnO films by confined dewetting lithography. Applied Surface Science, 2010, 256, 3386-3389.	6.1	12
107	Effect of ammonia on luminescent properties of YAG:Ce3+,Pr3+nanophosphors. , 2010, , .		1
108	Syntonized white up-converted emission by Tm ³⁺ -Yb ³⁺ -Er ³⁺ -Ho ³⁺ doped ZrO 2 nanocrystals. Proceedings of SPIE, 2010, , .	0.8	0

#	Article	IF	CITATIONS
109	Role of Yb3+ and Er3+ concentration on the tunability of green-yellow-red upconversion emission of codoped ZrO2:Yb3+–Er3+ nanocrystals. Journal of Applied Physics, 2010, 108, .	2.5	73
110	Brilliant blue, green and orange–red emission band on Tm3+-, Tb3+- and Eu3+-doped ZrO2nanocrystals. Journal Physics D: Applied Physics, 2010, 43, 465105.	2.8	38
111	Photovoltaic conversion enhancement of TiO 2 nanoparticles decorated with Au nanocrystals and sensitized with CdSe quantum dots and P3OT polymer. Proceedings of SPIE, 2010, , .	0.8	0
112	Role of the Hydrothermal Synthesis Conditions on the Structure and Morphology of Co-Doped Y ₂ O ₃ :Er ³⁺ -Yb ³⁺ Nanostructured Materials. Journal of Nano Research, 2010, 9, 109-116.	0.8	3
113	Nanoscience and Nanotechnology in Latin America. International Journal of Nanotechnology and Molecular Computation, 2010, 2, 38-76.	0.3	0
114	Influence of surface coating on the upconversion emission properties of LaPO4:Yb/Tm core-shell nanorods. Journal of Applied Physics, 2009, 105, 113532.	2.5	39
115	Green upconverted emission enhancement of ZrO ₂ : Yb ³⁺ –Ho ³⁺ nanocrystals. Journal Physics D: Applied Phys 2009, 42, 235105.	s i2.8 ,	8
116	Eu-Doped BaTiO3 Powder and Film from Sol-Gel Process with Polyvinylpyrrolidone Additive. International Journal of Molecular Sciences, 2009, 10, 4088-4101.	4.1	45
117	Synthesis of assembled ZnO structures by precipitation method in aqueous media. Materials Chemistry and Physics, 2009, 115, 172-178.	4.0	134
118	Surfactant effect on the upconversion emission and decay time of ZrO2:Yb-Er nanocrystals. Journal of Luminescence, 2009, 129, 449-455.	3.1	43
119	Effect of alkali metal oxides R2O (R=Li, Na, K, Rb and Cs) and network intermediate MO (M=Zn, Mg, Ba) Tj ETQq1	$1_{3.6}^{0.78431}$	4 rgBT /Ove 78
120	Structural and Chemical Characterization of Yb ₂ O ₃ -ZrO ₂ System by HAADF-STEM and HRTEM. Microscopy and Microanalysis, 2009, 15, 46-53.	0.4	11
121	Efficient photoluminescence of Dy3+ at low concentrations in nanocrystalline ZrO2. Journal of Solid State Chemistry, 2008, 181, 75-80.	2.9	85
122	Synthesis and photoluminescence of Y2O3:Yb3+–Er3+ nanofibers. Microelectronics Journal, 2008, 39, 551-555.	2.0	11
123	Enhancement of Upconversion Emission of LaPO ₄ :Er@Yb Coreâ^'Shell Nanoparticles/Nanorods. Journal of Physical Chemistry C, 2008, 112, 9650-9658.	3.1	153
124	Annealing effect on the luminescence properties of BaZrO3:Yb3+ microcrystals. Journal of Applied Physics, 2008, 104, .	2.5	16
125	Nitrogen-Doped and CdSe Quantum-Dot-Sensitized Nanocrystalline TiO ₂ Films for Solar Energy Conversion Applications. Journal of Physical Chemistry C, 2008, 112, 1282-1292.	3.1	192
126	Polarization microscopy with stellated gold nanoparticles for robust, in-situ monitoring of biomolecules. Optics Express, 2008, 16, 2153.	3.4	76

#	Article	IF	CITATIONS
127	Structural Characterization and Luminescence of Porous Single Crystalline ZnO Nanodisks with Sponge-like Morphology. Journal of Physical Chemistry C, 2008, 112, 240-246.	3.1	47
128	Er ³⁺ and Yb ³⁺ concentration effect in the spectroscopic properties and energy transfer in Yb ³⁺ /Er ³⁺ codoped tellurite glasses. Journal Physics D: Applied Physics, 2008, 41, 095102.	2.8	55
129	Comparison Between Isothermal Cold and Melt Crystallization of Polylactide/Clay Nanocomposites. Journal of Nanoscience and Nanotechnology, 2008, 8, 1658-1668.	0.9	24
130	Facile synthesis and optical applications of ceramic nanophosphors. , 2008, , .		0
131	Synthesis and Characterization of Amorphous SiO ₂ Nanowires Derived from a Polymeric Precursor. Journal of Nanoscience and Nanotechnology, 2008, 8, 997-1002.	0.9	10
132	Blue-green upconversion emission in ZrO2:Yb3+ nanocrystals. Journal of Applied Physics, 2008, 104, .	2.5	27
133	Biomolecule Assisted Hydrothermal Synthesis of Chainlike Network of Silver Sulfide Nanostructures. Journal of Nanoscience and Nanotechnology, 2008, 8, 986-992.	0.9	10
134	Second-harmonic imaging of ZnO nanoparticles. , 2007, , .		1
135	Structural and photoluminescence characterization of nanocrystalline YAG: Er3+prepared with the addition of PVA and UREA. , 2007, , .		1
136	Dopant concentration effect on the TL response of ZrO 2 :Lu ³⁺ nanocrystals under β-ray irradiation. Proceedings of SPIE, 2007, 6639, 79.	0.8	0
137	Fiber-Optic Chemical Sensor for Detection of NO2Using Poly (3-Octylthiophene). Fiber and Integrated Optics, 2007, 26, 335-342.	2.5	6
138	Enhancing the Up-Conversion Emission of ZrO ₂ :Er ³⁺ Nanocrystals Prepared by a Micelle Process. Journal of Physical Chemistry C, 2007, 111, 17110-17117.	3.1	22
139	Controlling the Growth and Luminescence Properties of Well-Faceted ZnO Nanorods. Journal of Physical Chemistry C, 2007, 111, 8489-8495.	3.1	186
140	Thermoluminescence properties of undoped and Tb3+ and Ce3+ doped YAG nanophosphor under UV-, X- and β-ray irradiation. Nuclear Instruments & Methods in Physics Research B, 2007, 255, 357-364.	1.4	22
141	Radiative and non radiative spectroscopic properties of Er3+ ion in tellurite glass. Optics Communications, 2006, 260, 601-606.	2.1	81
142	Concentration effect of Er3+ ion on the spectroscopic properties of Er3+ and Yb3+/Er3+ co-doped phosphate glasses. Optical Materials, 2006, 28, 560-568.	3.6	119
143	Absorption and refractive index changes of poly (3-octylthiophene) under NO2 gas exposure. Optical Materials, 2006, 29, 167-172.	3.6	17
144	Effect of the CTAB concentration on the upconversion emission of ZrO2:Er3+ nanocrystals. Optical Materials, 2006, 29, 31-37.	3.6	24

#	Article	IF	CITATIONS
145	NO 2 chemical oxidation doping effect on spin-coated poly(3-octylthiophene) thin films for NO 2 sensing applications. , 2005, , .		Ο
146	Strong Visible Cooperative Up-Conversion Emission in ZrO ₂ :Yb ³⁺ Nanocrystals. Journal of Nanoscience and Nanotechnology, 2005, 5, 1480-1486.	0.9	15
147	Thermoluminescence characterization of nanocrystalline and single Y3Al5O12 crystal exposed to β-irradiation for dosimetric applications. Optical Materials, 2005, 27, 1240-1244.	3.6	22
148	Low temperature synthesis and structural characterization of nanocrystalline YAG prepared by a modified sol–gel method. Optical Materials, 2005, 27, 1793-1799.	3.6	58
149	Nanoparticle thin films of nanocrystalline YAG by pulsed laser deposition. Optical Materials, 2005, 27, 1217-1220.	3.6	10
150	Synthesis, characterization and luminescence properties of ZrO2:Yb3+–Er3+ nanophosphor. Optical Materials, 2005, 27, 1295-1300.	3.6	69
151	Enhanced cooperative absorption and upconversion in Yb3+doped YAG nanophosphors. Optical Materials, 2005, 27, 1305-1310.	3.6	55
152	Luminescent properties and energy transfer processes of co-doped Yb–Er poly-crystalline YAG matrix. Optical Materials, 2005, 27, 1839-1844.	3.6	36
153	OSL and TL dosimeter characterization of boron doped CVD diamond films. Optical Materials, 2005, 27, 1231-1234.	3.6	6
154	Optically stimulated luminescence properties of nanocrystalline Y3Al5O12 phosphor exposed to β radiation. Optical Materials, 2005, 27, 1245-1249.	3.6	9
155	Visible light emission under UV and IR excitation of rare earth doped ZrO2 nanophosphor. Optical Materials, 2005, 27, 1320-1325.	3.6	105
156	Thermoluminescence and optically stimulated luminescence properties of nanocrystalline Er3+and Yb3+doped Y3Al5O12exposed to β-rays. Journal Physics D: Applied Physics, 2005, 38, 3854-3859.	2.8	23
157	Strong green upconversion emission in ZrO2:Yb3+–Ho3+ nanocrystals. Applied Physics Letters, 2005, 87, 241912.	3.3	123
158	Temperature effect in the crystallite size and the photoluminescence of nanocrystalline ZrO 2 :Sm3+phosphor. , 2004, , .		5
159	Concentration enhanced red upconversion in nanocrystalline ZrO2Â:ÂEr under IR excitation. Journal Physics D: Applied Physics, 2004, 37, 2489-2495.	2.8	41
160	Preparation, photo- and thermo-luminescence characterization of Tb3+ and Ce3+ doped nanocrystalline Y3Al5O12 exposed to UV-irradiation. Optical Materials, 2004, 25, 285-293.	3.6	49
161	Thermoluminescence characterization of Tb3+ and Ce3+ doped nanocrystalline Y3Al5O12 exposed to X- and β-ray irradiation. Optical Materials, 2004, 27, 293-299.	3.6	36
162	Concentration and crystallite size dependence of the photoluminescence in YAG:Ce3+nanophosphor. ,		4

2004, , .

#	Article	IF	CITATIONS
163	Luminescence and visible upconversion in nanocrystalline ZrO2:Er3+. Applied Physics Letters, 2003, 83, 4903-4905.	3.3	105
164	Influence of borate content on the radiative properties of Nd3+ ions in fluorophosphate glasses. Journal of Physics and Chemistry of Solids, 2003, 64, 69-76.	4.0	22
165	Monoclinic ZrO2 as a broad spectral response thermoluminescence UV dosemeter. Radiation Measurements, 2003, 37, 187-190.	1.4	51
166	Enhancement of optical properties of Nd3+ doped fluorophosphate glasses by alkali and alkaline earth metal co-doping. Optical Materials, 2003, 22, 201-213.	3.6	36
167	The red emission in two and three steps up-conversion process in a doped erbium SiO2–TiO2 sol–gel powder. Journal of Luminescence, 2003, 102-103, 504-509.	3.1	12
168	Luminescent properties and energy transfer in ZrO2:Sm3+ nanocrystals. Journal of Applied Physics, 2003, 94, 3509-3515.	2.5	95
169	Photoluminescence and thermoluminescence of YAG:Ce3+,Tb3+nanocrystalline under UV-, X- and $\hat{I}^2\text{-}irradiation.$, 2003, , .		3
170	Anisotropic media with orthogonal eigenpolarizations. Journal of Optics, 2002, 4, 419-423.	1.5	4
171	Refractive index measurement of pure and Er3+-doped ZrO2–SiO2 sol–gel film by using the Brewster angle technique. Optical Materials, 2002, 19, 275-281.	3.6	41
172	Luminescence and thermoluminescence induced by Gamma and UV-irradiation in pure and rare earth doped zirconium oxide. Optical Materials, 2002, 19, 195-199.	3.6	37
173	Nanocrystalline tetragonal zirconium oxide stabilization at low temperatures by using rare earth ions: Sm3+ and Tb3+. Optical Materials, 2002, 20, 263-271.	3.6	37
174	Stimulated emission and radiative properties of Nd3+ ions in barium fluorophosphate glass containing sulphate. Journal of Luminescence, 2002, 99, 141-148.	3.1	68
175	Loss measurements on laser-dye-doped and undoped unclad plastic optical fibers. , 2001, 4279, 183.		0
176	<title>Nonradiative energy transfer process in the system
Sm<formula><sup><roman>3</roman></sup></formula>+:
ZrO<formula><inf><roman>2</roman></inf></formula> prepared by sol-gel technique</title> . , 2001, ,		0
177	Fluorescence characterization of the ternary system TMQ-PBDBD365-POPOP-dye-doped polystyrene optical fiber under gamma and UV irradiation. , 2001, , .		0
178	Energy transfer in Tb:Nd system and composition dependence of the J-O parameters and radiative properties of Nd3+ions of fluorophosphate glasses. , 2001, , .		0
179	<title>Spectroscopic characterization of Nd<formula><sup><roman>3</roman></sup></formula>+
doped barium fluoroborophosphate and fluorosulphatephosphate glasses</title> ., 2001, , .		0
180	Spectroscopic characterization of Nd3+ ions in barium fluoroborophosphate glasses. Optical Materials, 2001, 18, 321-329.	3.6	36

#	Article	IF	CITATIONS
181	Characterization of Fluorescence Induced by Side Illumination of Rhodamine B Doped Plastic Optical Fibers. Fiber and Integrated Optics, 2001, 20, 457-464.	2.5	11
182	Evidence of non-radiative energy transfer from the host to the active ions in monoclinic ZrO2:Sm3+. Journal Physics D: Applied Physics, 2001, 34, L83-L86.	2.8	51
183	Plastic optical fiber technology. , 2000, , .		1
184	Plastic optical fibers with in-line electrode structures. , 2000, , .		0
185	Luminescence characterization of rhodamine-B-doped plastic optical fibers using the side induced fluorescence method. , 2000, 4106, 62.		1
186	Thermo-luminescence induced by gamma irradiation in sol-gel prepared zirconia-silica materials. Materials Research Innovations, 2000, 4, 32-35.	2.3	4
187	High temperature thermoluminescence induced on UV-irradiated tetragonal ZrO2 prepared by sol–gel. Materials Letters, 2000, 45, 241-245.	2.6	52
188	Temperature-Induced Changes of Sensitivity in the Unbalanced Hi-Bi Fiber Sagnac Interferometer. Fiber and Integrated Optics, 1999, 18, 41-48.	2.5	5
189	All-fiber absolute temperature sensor using an unbalanced high-birefringence Sagnac loop. Optics Letters, 1997, 22, 481.	3.3	100
190	Fiber Sagnac interferometer temperature sensor. Applied Physics Letters, 1997, 70, 19-21.	3.3	182
191	Cooperative Pair Driven Quenching of Yb ³⁺ Emission in Nanocrystalline ZrO ₂ :Yb ³⁺ . Journal of Nano Research, 0, 5, 121-134.	0.8	8